

University of Groningen

How to escape from a tense situation

Folgering, Jozef Hendrik Arnold

IMPORTANT NOTE: You are advised to consult the publisher's version (publisher's PDF) if you wish to cite from it. Please check the document version below.

Document Version

Publisher's PDF, also known as Version of record

Publication date:

2005

[Link to publication in University of Groningen/UMCG research database](#)

Citation for published version (APA):

Folgering, J. H. A. (2005). *How to escape from a tense situation: Bacterial mechanosensitive channels*. s.n.

Copyright

Other than for strictly personal use, it is not permitted to download or to forward/distribute the text or part of it without the consent of the author(s) and/or copyright holder(s), unless the work is under an open content license (like Creative Commons).

The publication may also be distributed here under the terms of Article 25fa of the Dutch Copyright Act, indicated by the "Taverne" license. More information can be found on the University of Groningen website: <https://www.rug.nl/library/open-access/self-archiving-pure/taverne-amendment>.

Take-down policy

If you believe that this document breaches copyright please contact us providing details, and we will remove access to the work immediately and investigate your claim.

Downloaded from the University of Groningen/UMCG research database (Pure): <http://www.rug.nl/research/portal>. For technical reasons the number of authors shown on this cover page is limited to 10 maximum.

***Lactococcus lactis* uses MscL as its principal mechanosensitive channel**

Joost H.A. Folgering, Paul C. Moe, Gea K. Schuurman-Wolters, Paul Blount and Bert Poolman

This chapter was published: (2005) *J. Biol. Chem.* **280**, 8784-92

Abbreviations: GUV: Giant Unilamellar Vesicle; MTSET: [2-(trimethylammonium)ethyl] methanethiosulfonate; ITO: Indium-Tin-Oxide; NTA: Nitrilo-Triacetic Acid; CFU: Colony Forming Units; GOF: Gain-Of-Function; MS: Mechano-Sensitive; CDM: Chemically Defined Medium; RT-PCR: Reverse Transcription - Polymerase Chain Reaction

Abstract

The functions of the mechanosensitive channels from *Lactococcus lactis* were determined by biochemical, physiological and electrophysiological methods. Patch-clamp studies showed that the genes *yncB* and *mscL* encode MscS and MscL-like channels, respectively, when expressed in *E. coli* or if the gene products were purified and reconstituted in proteoliposomes. However, unless *yncB* was expressed in *trans*, membranes derived from wild-type of *Lactococcus lactis* displayed only MscL activity. Membranes prepared from a *mscL* disruption mutant did not show any mechanosensitive channel activity, irrespective of whether the cells had been grown on low or high osmolarity medium. In osmotic downshift assays, wild-type cells survived and retained 20% of the glycine betaine internalized under external high salt conditions. On the other hand, the *mscL* disruption mutant retained 40% of internalized glycine betaine and was significantly compromised in its survival upon osmotic downshifts. The data strongly suggest that *Lactococcus lactis* uses MscL as the main mechanosensitive solute-release system to protect the cells under conditions of osmotic downshift.

Introduction

Mechanosensitive channels play an important role in prokaryotic cell volume regulation (1). In small, single-cell, organisms this regulation can mean the difference between life and death under extreme osmotic downshift conditions. By diffusion over the semi-permeable cell membrane and/or aquaporins embedded in the membrane, water can enter and leave the cell until equilibrium is established between internal and external osmolality. This allows microorganisms to adapt to changes in external osmolyte concentrations. When the external osmolyte concentrations increase (hyperosmotic stress), water will leak out of the cell, causing loss of turgor and ultimately the cell may plasmolyse. Bacteria respond to this hyperosmotic stress by rapid uptake of ions (K^+) and/or compatible solutes or increasing the intracellular osmolyte concentration through synthesis of compatible solutes. The increase in internal compatible solute concentration compensates for the

high external osmolality allowing water to diffuse back and the cell to regain its original volume and turgor (2-4).

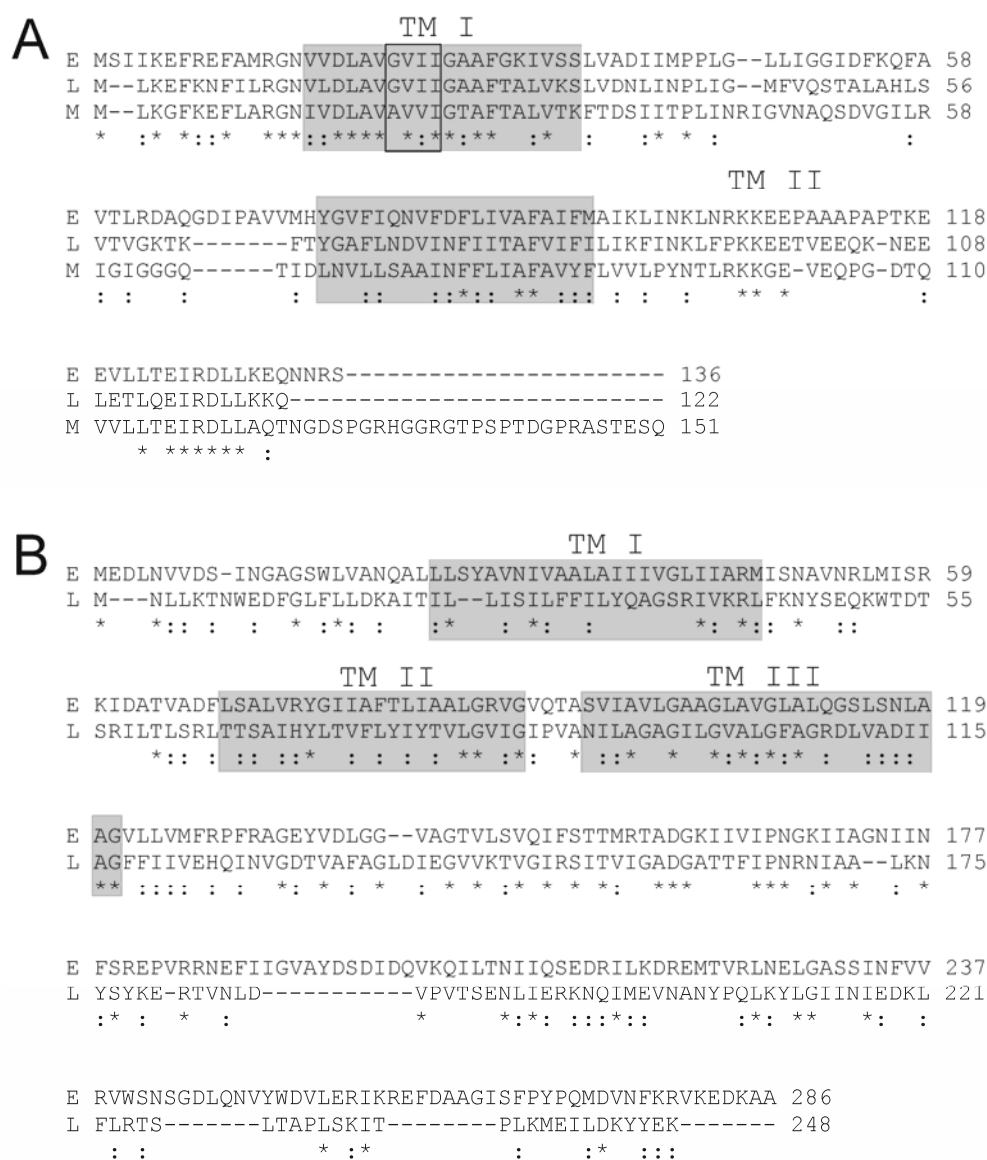


Figure 1: (A) Alignment of MscL from *E. coli* (E), *L. lactis* (L) and *M. tuberculosis* (M). The boxed α -amino acids in panel A correspond to the positions of the cysteine mutants. (B) Alignment of MscS from *E. coli* (E) and *L. lactis* (L). The homology between the proteins is indicated as follows: (*) fully conserved residues, (:) close conservative substitutions. The transmembrane segments are shaded grey.

Conversely, when the external osmolyte concentration suddenly decreases, water will diffuse into the cell causing it to swell and, in extreme conditions, lyse. This is where the mechanosensitive channels are thought to play a role by opening in response to the increased membrane tension effected by the rapid increase in cell volume. The best-known example of a channel in this role is the Mechanosensitive Channel of Large conductance

from *E. coli* (MscL^{Ec}), but homologues are present in most eubacteria (5-7). MscL opens near the lytic tension limit of the bacterial membrane. A second mechanosensitive channel, that of small conductance, MscS, has been characterized in only a few organisms (8, 9). MscS opens at lower membrane tensions and has a smaller conductance than MscL, making it useful for fine-regulation of internal compatible solute concentration. Crystal structures of MscL and MscS are available (10, 11). The electrophysiological characteristics of MscS from *E. coli* (12) and of a number of MscL homologues (5) have been described. So far their physiological roles in osmoprotection are not fully understood.

Previously we have established the mechanism of the osmotic regulation of the upshift activated glycine betaine transporter OpuA from *Lactococcus lactis* (13, 14). Although the physicochemical properties of the membrane and lipid-protein interactions also play a critical role in the osmotic activation of OpuA, the mechanism is entirely different from that underlying the gating of MS channels. We have shown that increasing internal ionic strength, a consequence of osmotic upshift, activates OpuA by altering the electrostatic interactions between anionic lipids and charged residues at the cytoplasmic face of the protein (15). For a better understanding of the total osmoregulatory response of *L. Lactis*, we present here the electrophysiological and biochemical characterization of *L. lactis* MscL (MscL^{Ll}; 45.4% identity with MscL^{Ec}; Fig 1A) and YncB (hereafter referred to as MscS^{Ll}; 24.0% identity with MscS from *E. coli*; Fig 1B) and show that MscL^{Ll} is critical for protection of *L. lactis* against osmotic downshifts. In fact, the majority of glycine betaine, accumulated upon upshift activation of OpuA, seems to exit the cell via MscL^{Ll} upon subsequent osmotic downshift. We also examined the expression of the *opuA*, *mscL* and *yncB* genes during cell growth under low and high salt conditions.

Table 1: Bacterial strains and their relevant genotypes

Strain	Relevant genotype	Reference
<i>E. coli</i>		
PB104	<i>E. coli</i> AW405, $\Delta mscL::Cm^{res}$ <i>recA</i> ⁻	16
MJF465	<i>E. coli</i> Frag1, $\Delta mscL::Cm^{res}$, $\Delta yggB$, $\Delta kefA::kan^{res}$	12
JM110	<i>dam</i> ⁻ , <i>dcm</i> ⁻	17
<i>L. lactis</i>		
IL1403	Plasmid free strain	18
MG1363	Plasmid free strain	19
NZ9000	MG1363 <i>pepN::nisR nisK</i>	20
JIM7049	IL1403 <i>his::nisR nisK</i>	21
JIM7049 Δ MscL	IL1403 <i>his::nisR nisK</i> ; <i>MscL::Em</i> ^{res}	This work
LI108	<i>RepA</i> ⁺ MG1363, carrying multiple copies of pWVO1 <i>repA</i> in the chromosome, <i>Cm</i> ^{res+}	22

Table 2: List of plasmids used in this study and their characteristics

Plasmid	Relevant characteristics	Reference
pBlueScript	β -galactosidase α -complementation; <i>Xba</i> I, <i>Xho</i> I in multiple cloning site; <i>Amp</i> ^{res}	23
pB10b	pBR322 <i>ori</i> ; <i>lacUV5</i> promoter; <i>Xba</i> I, <i>Xho</i> I in multiple cloning site; <i>Amp</i> ^{res}	16
pBAD	pBR322 <i>ori</i> ; <i>P</i> _{BAD} promoter; <i>Nco</i> I, <i>Hind</i> III in multiple cloning site; <i>Amp</i> ^{res}	24
pB10bmScL ^{L1}	pB10b with <i>L. lactis mscL</i> inserted in <i>Xba</i> I, <i>Xho</i> I	This work
pB10bmScL ^{L1} 6H	pB10b with <i>L. lactis mscL</i> , and sequence coding for a C-terminal 6-histidine tag, inserted in <i>Xba</i> I, <i>Xho</i> I	This work
pB10bmScL ^{L1} 6H G20C	pB10BMscLLI6H G20C	This work
pB10bmScL ^{L1} 6H V21C	pB10BMscLLI6H V21C	This work
pB10bmScL ^{L1} 6H I22C	pB10BMscLLI6H G22C	This work
pB10bmScL ^{L1} 6H I23C	pB10BMscLLI6H V23C	This work
pBADyncB10H	pBAD with <i>L. lactis yncB</i> , and sequence coding for a C-terminal 10-histidine tag, inserted; in <i>Nco</i> I, <i>Hind</i> III	This work
pET324	pBR322 <i>ori</i> ; <i>lacUV5</i> promoter; <i>Nco</i> I, <i>Hind</i> III in multiple cloning site; <i>Amp</i> ^{res}	25
pET324yncB10H	pET324 with <i>L. lactis yncB</i> , and sequence coding for a C-terminal 10 histidine tag inserted; in <i>Nco</i> I, <i>Hind</i> III	This work
pNZ8020	pSH71 replicon; <i>nisA</i> promoter; <i>Xba</i> I <i>Xho</i> I in multiple cloning site; <i>Cm</i> ^{res}	20
pNZ8020mScL ^{L1} 6H	pNZ8020 with <i>L. lactis mscL</i> , and sequence coding for a C-terminal 6-histidine tag; inserted in <i>Xba</i> I, <i>Xho</i> I	This work
pNZ8048	pSH71 replicon; <i>nisA</i> promoter, <i>Nco</i> I, <i>Hind</i> III in multiple cloning site; <i>Cm</i> ^{res}	26
pNZ8048yncB10H	pNZ8048 with <i>L. lactis yncB</i> , and sequence coding for a C-terminal 10-histidine tag; inserted in <i>Nco</i> I, <i>Hind</i> III	This work
pOri280	pWV01-derivative; <i>repA</i> ⁺ , replicates only in strains that carry <i>repA</i> in <i>trans</i> ; <i>Em</i> ^{res}	22
pOri280 Δ MscL ^{L1}	pOri280 with an internal fragment of <i>mscL</i> ^{L1} inserted in <i>Xba</i> I, <i>Bam</i> HI; <i>Em</i> ^{res}	This work

Materials and Methods

Strains, plasmids and growth conditions

Experiments were performed using the strains listed in Table 1 and plasmids listed in Table 2. *Escherichia coli* strains were grown in Luria broth, with 100 μ g/ml ampicillin when required. *Lactococcus lactis* cells were grown in M17 broth (Difco) or chemically defined medium (27) supplemented with 25mM glucose and 365mM KCl for high salt conditions (1050mOsmol/kg).

Chloramphenicol (5µg/ml) or erythromycin (5µg/ml) was added when the cells were transformed with plasmids. For growth on solid medium 1.5% (w/v) agar was added to the broth.

Cloning of *mscL* and *yncB*

The primers that were used for the amplification of *mscL* and *yncB* are listed in Table 3. As the *yncB* gene product is homologous to MscS from *E. coli*, and functions similarly, the YcnB protein is referred to as MscS^{LI}. The superscripts LI and Ec will be used to denote genes or proteins from *L. lactis* and *E. coli*, respectively. For PCR amplifications, Expand High-Fidelity DNA polymerase (Roche) was used and reactions were performed according to the manufacturer's instructions. Chromosomal DNA of *L. lactis* IL1403 was used as template, the annealing temperature was 50°C for *mscL*^{LI} and 53°C for *yncB*, and the elongation times were 30 and 60 sec, respectively. For the histidine-tagged version of MscL^{LI}, a two step PCR was performed using primers LL.SD.5' and LL.SD.4H3' (see Table 3) to introduce a 4-histidine tag, and then a second step was used to engineer another two histidines, a stop codon and a restriction site for cloning.

Table 3: Primers used in this study

Name	Sequence
FW WT MscL ^{LI}	5' - TCTAGATCTAGATATTATATAGGATTTATGTTAA
REV WT MscL ^{LI}	5' - GAGCTCGAGCTCGGGCTAGAGGGAGTTTGGTTAGC
LL.SD.5'	5' - TCTAGATCTAGAAGGAGGAGCCATGGTAAAGGAATTTAAAAAC
LL.SD.4H3'	5' - GTGATGGTGATGTTGTTTTTTCAATAAATCGCGAATTTTC
LL.SD.6H3'	5' - CTCGAGCTCGAGTTAGTGATGGTGATGGTGATGTTGTTTTTTCAATA
<i>yncB</i> FW	5' - ATATATCCATGGACTTATTA AAAACAAACTGGGAA
<i>yncB</i> REV	5' - ATATATAAGCTTAATGGTGATGGTGATGGTGTTTTTTCATAATATTTA TCTAAAATCTCC
G20C	5' - GGGAACGTATTGGACTTAGCCGTTTGTGTTATCATCGGGGCAG
V21C	5' - GGGAACGTATTGGACTTAGCCGTTGGGTGTATCATCGGGGCAG
I22C	5' - GGGAACGTATTGGACTTAGCCGTTTGTGTTTGTATCGGGGCAG
I23C	5' - GGGAACGTATTGGACTTAGCCGTTGGGGTTATCTGTGGGGCAG
DIS FW	5' - CTGGCGTCTAGAGGGAACGTATTGGACTTAGCCG
DIS REV	5' - CCGGCCGATCCAAGAATGAAAATAACAAAGGC
RT-YncB fw	5' - CTCTATCAAGCCGGCTCTCG
RT-YncB rev	5' - GAGGGCAGCAATATTTTCGATTAGG
RT-MscL fw	5' - GGGAACGTATTGGACTTAGCCG
RT-MscL rev	5' - CGCGAATTTCTTGGAGAGTTTCC
RT-Opu fw	5' - CGCGCAGAGAAGGCCTTAG
RT-Opu rev	5' - CAGCCATTAGAGAGCTGACC

The *mscL*^{LI} and *mscL*^{LI6H} genes were first sub-cloned in pBluescript, isolated from *E. coli* JM110, using the *XhoI*-*XbaI* restriction sites. This construct was used to transform JM110, and after plasmid isolation, the genes were excised from the pBluescript vector and ligated into pNZ8020 and pB10b again using the *XhoI*-*XbaI* restriction sites. The resulting plasmids

pNZ8020m scL^{LI} 6H and pB10bm scL^{LI} were then used to transform *L. lactis* JIM7049 and *E. coli* PB104, respectively. *YncB10H* was ligated directly after PCR into the vectors pNZ8048, pET324 and pBAD and used to transform *L. lactis* IL1403 and *E. coli* JM465, respectively. Finally, all constructs were mid-prepped (Qiagen) and the DNA sequence was analyzed to confirm fidelity.

Construction of single cysteine mutants and a *L. lactis mscL* disruption strain

The primers used for the construction of the mutants of M scL^{LI} are listed in Table 3. The cysteine mutants were constructed using pB10bm scL^{LI} 6H as template. First, LL.SD.6H3' was combined with the primer for the specific mutant to create a megaprimer, which in a second amplification step was combined with LL.SD.5' to obtain the complete *mscL* sequence with the desired cysteine modification. All other conditions were as described above for the cloning of M scL 6H.

For the construction of the *L. lactis* JIM7049 *mscL* disruption strain, an internal gene fragment, from codon 12 to codon 86, was amplified. From earlier studies with truncation mutants of *E. coli* M scL , it could be predicted that a disruption with this gene fragment should lead to complete inactivation of M scL (28). The amplification was performed using the same conditions as described above for amplification of *mscL*6H. The internal gene fragment was ligated in pOri280, using the *Xba*I and *Bam*HI restriction sites. The vector was hosted in *L. lactis* LI108 for propagation of the plasmid and, after confirmation of the DNA sequence, the plasmid was introduced into *L. lactis* JIM7049. The cells were grown on M17-glucose solid medium, supplemented with erythromycin (5 μ g/ml) to select for colonies that harboured the plasmid DNA integrated into the chromosome (22). The *mscL* disruption strain is designated JIM7049 Δ M scL .

Transcriptional analysis

Cells were grown to mid-exponential phase of growth on CDM and diluted 1:1 to CDM without NaCl or CDM plus 0.5M NaCl (final concentration), and harvested 10 minutes after dilution. RNA was extracted as described (29) at concentrations of 4-5 μ g/ μ l. The RNA was used as template for the AMV reverse transcriptase, using the 1st strand cDNA synthesis kit for RT-PCR (Roche Applied Science, Indianapolis), according to the manufacturer's instructions and in the presence of the supplied random hexanucleotide primers. The obtained cDNA was subsequently used as template in a PCR reaction with Taq polymerase using the RT-M scL , RT-M scS and RT-OpuA forward (fw) and reverse (rev) primers listed in Table 3. The primers were designed to amplify internal gene fragments of 316 (bp 34 - 349 of *mscL*), 418 (bp 94 - 513 of *yncB*) and 502 (bp 430 - 931 of *opuAA*) basepairs.

For PCR amplification, the annealing temperature was 50°C and the elongation time was 60sec. The products were analyzed on a 1.5% agarose gel after 15 and 25 cycles. As a control, the PCR was also performed on chromosomal DNA of *L. lactis*; as a negative control the RNA samples were treated in exactly the same manner, except that the AMV reverse transcriptase was omitted in the reaction with RNA as template.

Preparation of MS channel-containing membranes for patch clamp analysis

Hybrid proteo-GUVs. *L. lactis* NZ9000 containing pNZ8020mScL^{LI}6H was grown in M17-glucose medium to an OD₆₀₀ of 0.8, after which *mScL* expression was induced for three hours with a 1:1000 dilution of the supernatant of a culture from the nisinA producing *L. lactis* NZ9700 strain (20). Inside-out membrane vesicles were prepared by lysing the bacteria (20mg/ml protein) with a high-pressure homogenizer (Kindler type NN2002; single passage at 10,000psi), following (partial) digestion of the cell wall with 10mg/ml lysozyme for 30min at 30°C. After removing unlysed cells and cell wall debris by centrifugation at 20,000xg, the membrane vesicles were washed once by centrifugation at 150,000xg and then resuspended in 50mM KPi, pH 6.5. Aliquots of 0.5ml were frozen in liquid nitrogen and stored at -80°C. The membrane vesicles were mixed with liposomes (2:25 w/w total membrane protein/lipid ratio), centrifuged at 270,000xg and resuspended in 5% ethylene glycol and dehydrated on a glass slide. To obtain fused proteo-GUVs rehydration was performed by placing rehydration buffer (200mM KCl, 0.1mM EDTA, 0.01mM CaCl₂ plus 5mM HEPES, pH 7.2) on top of the dried membranes to obtain a final lipid concentration of 100mg/ml as described (30). Alternatively, after drying on glass slides coated with indium tin oxide (ITO), hybrid proteo-GUVs were obtained by rehydration in a flow chamber with 300µl of 10mM KCl, 2mM MgCl₂, 0.25mM HEPES, pH 7.2 plus 320mM sucrose (the sucrose was added to make the rehydration medium equiosmolar to the buffer for patch-clamp analysis). The flow chamber was closed with a second ITO-coated glass slide. A voltage of 1.2V at 10Hz was applied for at least 3h through electrodes sealed on the glass plates. The resulting giant unilamellar vesicles (GUVs), 5-50µm in diameter, were used in patch clamp experiments (31).

Proteo-GUVs. Membrane vesicles, containing overexpressed channel protein (MscL^{LI} or MscS^{LI}), were solubilized in 50mM KPi, 35mM imidazole, 300mM NaCl, pH 7.0 plus 3% octyl-β-D-glucoside (Anatrace) at 4°C for 20 min and under continuous stirring of the suspension. The solubilized proteins and remaining membrane material were separated by ultracentrifugation at 270,000xg for 20min at 4°C. The supernatant was then loaded onto Ni-NTA affinity resin pre-equilibrated with solubilization buffer. The column was washed with 20-30 volumes of solubilization buffer containing 0.5% Triton X-100, after which the proteins were eluted with 50mM KPi, 300mM NaCl, pH 7.0 plus 0.2% Triton X-100 with a step gradient of imidazole. The purified proteins were mixed with Triton X-100-destabilized preformed liposomes (10mg/mL of lipid); the lipid mixtures were composed of dioleoyl 18:1 (Δ9 cis) phospholipids, that are, DOPC, DOPE and/or DOPS, typically at protein-to-lipid ratios of 1 to 2,000-20,000 (mol monomeric channel protein per mol lipid), and reconstitutions were performed as described (32). The proteoliposomes were converted to proteo-GUVs by dehydration and rehydration in the presence or absence of an electrical field, as described under "*Hybrid proteo-GUVs*".

Spheroplasts. For determination of pressure ratios, relative to MscS^{Ec}, of MscL^{L1} and the individual cysteine mutants, giant spheroplasts were prepared from *E. coli* PB104 containing pB10bmScL^{L1}6H or its derivatives. For other channel characteristics giant spheroplasts were prepared from *E. coli* MJF465 containing pB10bmScL^{L1}, pB10bmScL^{L1}6H or pET324yncB10H. All spheroplasts were prepared as described (30).

Patch clamp experiments

Experiments were performed as described previously (30). After preparation, an aliquot of proteo-GUVs or 1-5 μ l of a spheroplast sample was transferred to a sample chamber containing a ground electrode and 300 μ l of patch clamp buffer: 5mM HEPES, pH 7.2, 200mM KCl plus 40mM MgCl₂ for proteo-GUVs; 5mM HEPES, pH 7.2, 200mM KCl, 90mM MgCl₂, plus 10mM CaCl₂ for spheroplasts. Channel activity was recorded using an Axopatch 200A amplifier together with a digital converter and Axoscope software (Axon Instruments, Foster City, USA). Data were acquired at a sampling rate of 33kHz and filtered at 10kHz. The presented traces were additionally filtered to decrease electronic noise, using Clampfit 8.0 software (Axon Instruments, Foster City, USA) with the lowpass Boxcar filter at smoothing point 7. Offline analysis was performed using PClamp 6.0 software (Axon Instruments, Foster City, USA).

Glycine betaine efflux

Glycine betaine efflux was performed as described (13) with some modifications. Cells were grown overnight to late log phase in high osmolality medium (1050mOsmol/kg) and washed 3 times in their original volume with an equiosmolar buffer (50mM KPi, 500mM KCl, pH 6.5). The cells were then resuspended to a protein concentration of ~10mg/ml and stored on ice. For uptake of glycine betaine, the cells were diluted 10-fold in 50mM KPi, pH 6.5, 500mM KCl, supplemented with 10mM glucose and 1.88mM of [¹⁴C]-glycine betaine. After 40 minutes of uptake at 30°C, aliquots of the cells were subjected to no dilution or 3, 5, 10, 20, 50 and 100-fold dilution into 50mM KPi, pH 6.5. This resulted in final osmolalities of 1050, 420, 295, 200, 155, 125 and 115mOsmol/kg, respectively. Samples were taken in five-fold, to determine the steady state internal glycine betaine concentrations prior to the osmotic downshift (final internal glycine betaine content) and at different time intervals (at 1 [in duplicate], 5, 10 and 30 minutes) after each of the downshifts. At least three independent uptake and downshift experiments were performed on three independent cultures of *L. lactis* IL1403 and JIM7049 Δ MscL. The steady state levels of internalized glycine betaine after uptake were ~900nmol/mg protein for both strains. Release is plotted as a percentage of retained glycine betaine.

Analysis of cell viability

Survival of *E. coli* MJF465, carrying pB10bmScL^{L1}6H, pET324yncB10H or empty plasmid controls, under osmotic downshift conditions, was analyzed as described (12). Because *E. coli* MJF465 is not able to use arabinose as an energy source and glucose represses the expression of the arabinose inducible-system, the IPTG-inducible construct pET324yncB10H was used

here. The cysteine mutants were screened for survival with, and without, MTSET as described (33). For survival under osmotic downshift conditions of *L. lactis* IL1403 or JIM7049 Δ MscL, cells were grown overnight in chemically defined medium (27), supplemented with 25mM glucose and 5 μ g/ml erythromycin (where applicable) and diluted 1:100 to the same medium supplemented with 365mM KCl (1050mOsmol/kg). Cells were allowed to grow to OD₆₀₀ of ~0.8 and then diluted 100-fold into 50mM KPi, pH 6.5 plus 500mM KCl (1050mOsmol/kg) or into 50mM KPi, pH 6.5 (final osmolality of 115mOsmol/kg). Prior to plating onto agar containing media, the cells were diluted serially with sterile equiosmolar buffers, all prewarmed to 30°C. To determine cell viability, 20 μ l samples were spotted onto equiosmolar CDM agar plates, and incubated for 36h at 30°C before the number of colony forming units (CFU) was determined.

Metabolic activity after osmotic downshift

Because *L. lactis* grows in chains, the number of CFU is not necessarily a quantitative indicator of the survival of cells after downshift. Therefore, metabolic activity based on the production of acid by *L. lactis* during fermentation of glucose was also determined. The method was adapted from (34). In brief: cells were cultured, washed and osmotically-stressed as described above for the glycine betaine efflux assay, but with 5mM KPi, pH 6.5 plus 65mM KCl (105mOsmol/kg) instead of 50mM KPi buffer (105mOsmol/kg) to reduce the buffering capacity. Acidification rates per mg total protein in the presence of 10mM glucose were determined for all samples and compared with the acidification rates of the unshocked sample (100% value).

Miscellaneous

Protein biochemistry. Purified proteins were analyzed on 15% acrylamide SDS-PAGE (35). Protein concentration was determined by Amido-black 10B staining as described (36). MscL was also identified and analysed for potential modifications or proteolysis products by MALDI-TOF mass spectrometry as described (37). The MscL⁻ phenotype of *L. lactis* JIM7049 Δ MscL was checked by preparation of cell membranes, and subsequent SDS-PAGE analysis. The presence or absence of MscL^{L1} was determined by immuno-detection using specific rabbit serum with polyclonal antibodies raised against MscL^{L1} (at a titer of 1:30,000) and the Western-light chemiluminescence detection kit (Tropix Inc., Bedford, MA.).

Determination of osmolality. Osmolalities of media and buffers were measured by freezing point depression with an Osmostat 030 (Gonotec, Berlin).

Results

Cloning, Expression and Purification

Cloning and expression of *mscL*^{L1} and *yncB*^{L1} was achieved both in *E. coli* (not shown) and *L. lactis* (Fig. 2A). For amplification of MscL^{L1} and MscS^{L1} in *L. lactis* the nisin-inducible expression system was used (38). In *E. coli* the *lacUV5* promoter system was used for amplification of MscL^{L1} and the

arabinose-inducible system for amplification of MscS (24). MscL^{LJ}-6H and MscS^{LJ}-10H were purified by Ni-NTA chromatography. Based on the yield of purified protein, both channels were found to be amplified in *L. lactis* to levels between 5 and 10% and in *E. coli* between 2 and 5% of total membrane protein.

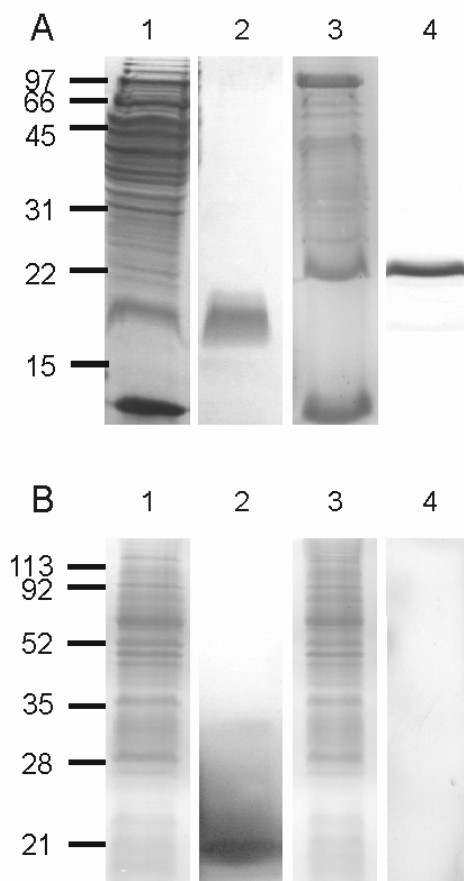


Figure 2: Overexpression, purification and immunodetection of MscL^{LJ} and MscS^{LJ}. (A) Coomassie brilliant blue-stained gel; lane 1: JIM7049, pNZ8020mScL^{LJ}6H membrane vesicles, lane 2 purified MscL^{LJ}, lane 3: JIM7049, pNZ8048yncB10H membrane vesicles, and lane 4: purified MscS^{LJ}. SDS-PAGE analysis of purified MscL^{LJ} showed a remarkably broad band, which could not be refined by boiling of the samples prior to SDS-PAGE analysis. Mass-spectrometry analysis showed the MscL^{LJ} band in the gel contained only full length MscL^{LJ}. (B) lane 1: coomassie brilliant blue-stained gel of IL1403 membranes, lane 2: immunoblot of IL1403 membranes, using MscL^{LJ}-specific antibodies, lane 3: coomassie brilliant blue-stained gel of JIM7049ΔMscL^{LJ} membranes, and lane 4: immunoblot of JIM7049ΔMscL^{LJ} membranes, using MscL^{LJ} specific antibodies.

As can be seen in Fig. 2A and B, MscL^{LJ} protein amplified in and purified from *L. lactis* NZ9000 migrated over a wide range in SDS-PAGE and gave rise to a ‘fuzzy’ appearance. To establish the nature of the differently migrating species, various fractions from the gel were analyzed by MALDI-TOF mass spectrometry. Four distinct slices of the gel were digested with CNBr and trypsin and the resulting peptide fragments were identified. The

fragments of the protein, after cleavage, accounted for 70% of the total protein (data not shown) including both the N and C termini, indicating that the heterogeneity observed on the gel was not due to proteolytic degradation of the amplified protein. We suggest that the broad and fuzzy band reflects incomplete unfolding of the protein in the presence of SDS, or a very strong association between individual subunits, which is only dissociated during SDS-PAGE analysis.

In vivo complementation of *E. coli* MJF465 (*MscL*⁻ / *MscS*⁻)

For initial characterization of *MscL*^{L1} and *MscS*^{L1}, the corresponding genes were expressed in *E. coli* MJF465 (*MscL*⁻/*MscS*⁻), using plasmids pB10bm*scL*^{L1}6H and pET324y*ncB*10H. This allowed a comparison of the ability of the *L. lactis* and *E. coli* channels to rescue the osmotic-fragile phenotype of *E. coli* MJF465 (12). Clearly both *MscL*^{L1} and *MscS*^{L1} were able to rescue MJF465 in osmotic downshift experiments (Table 4), albeit not as well as the endogenous *E. coli* channels.

Table 4: Survival of *E. coli*

Strain	Plasmid	Stress	Survival % (s.e.m.)	
MJF465	pB10b / pET324	osmotic downshift	0.6	(0.3)
MJF465	pB10bm <i>scL</i> ^{Ec} 6H	osmotic downshift	90.0	(4.5)
MJF465	pB10bm <i>scL</i> ^{L1} 6H	osmotic downshift	35.3	(3.2)
MJF465	<i>pyggb2</i>	osmotic downshift	78.0	(4.0)*
MJF465	pET324y <i>ncB</i> 10H	osmotic downshift	27.1	(1.9)
PB104	pB10bm <i>scL</i> ^{L1} 6H	–	100.0	(def)
PB104	pB10bm <i>scL</i> ^{L1} 6H	MTSET	100.0	(2.8)
PB104	pB10bm <i>scL</i> ^{L1} 6H G20C	MTSET	0.1	(0.1)
PB104	pB10bm <i>scL</i> ^{L1} 6H V21C	MTSET	1.0	(3.0)
PB104	pB10bm <i>scL</i> ^{L1} 6H I22C	MTSET	100.0	(1.7)
PB104	pB10bm <i>scL</i> ^{L1} 6H I23C	MTSET	100.0	(2.2)

* after (12)

Survival upon osmotic downshift of *E. coli* MJF465 (*MscL*⁻ / *MscS*⁻) carrying plasmids for *MscL*^{Ec} (pB10bm*scL*^{Ec}6H), *MscL*^{L1} (pB10bm*scL*^{L1}6H), *MscS*^{Ec} (*pyggb2*), *MscS*^{L1} (pET324y*ncB*10H) or empty plasmid controls (pB10B, pET324). Survival upon modification with MTSET (1mM, final concentration) of *E. coli* PB104 (*MscL*⁻) carrying pB10bm*scL*^{L1}6H or one of the derived cysteine mutants pB10bm*scL*^{L1}6H G20C, pB10bm*scL*^{L1}6H V21C, pB10bm*scL*^{L1}6H I22C or pB10bm*scL*^{L1}6H I23C. 100% survival was set for unchallenged cells. For all values, n≥3.

It has been demonstrated that *MscL*^{Ec} can be activated by MTSET modification of a cysteine introduced at position 22 (33, 39, 40). The equivalent residue, G20, in *MscL*^{L1} and its flanking residues (V21, I22 and I23; boxed region in Fig. 1) were replaced by cysteines and the phenotype of the

mutants, upon labeling with MTSET, was determined (Table 4). The cysteine positions that showed a clear GOF phenotype as a result of increased channel activity after reaction with MTSET under iso-osmotic conditions, G20C and V21C (equivalent to positions G22C and V23C in MscL^{Ec}), were further characterized in patch clamp experiments.

Electrophysiological characterisation

MscS^{Ll} in E. coli. Channel activity of an excised patch from *E. coli* MJF465 expressing MscS^{Ll}10H (from pBADyncB10H) is shown in Fig. 3A. The slope of the current-voltage relationship in Fig. 4A indicates that MscS^{Ll} allows a conductance of 0.87 ± 0.07 nS. The fact that the data in Fig. 4A could be fit to a straight line reveals that the channel shows no rectification between -50 mV and 50 mV. Open dwell-times of one to several hundreds of ms were observed and the channel appeared to desensitize when pressure was maintained for longer periods of time ($n=5$). Overall, the channel characteristics of MscS^{Ll} are analogous to those previously described for MscS from *E. coli* (12).

MscL^{Ll} in E. coli. Channel activity of an excised patch from *E. coli* MJF465, expressing MscL^{Ll}6H (from pB10bmscL6H) is shown in Fig. 3B. The current-voltage relationship for MscL^{Ll} (Fig. 4A) shows that MscL^{Ll} has a conductance of 2.00 ± 0.25 nS. Also, MscL^{Ll} did not show rectification between -50 mV and 50 mV. Two short but distinct dwell times were observed in 34 independent recordings (both from lipid fusions and spheroplasts; Fig. 4B). One dwell time could be determined at 3.6 ± 0.29 ms (mean and s.e.m.), the second was shorter than 1 ms and could not be determined more accurately given the experimental parameters. These dwell times are comparable to the dwell times of MscL from *Staphylococcus aureus* and are shorter than the dwell times observed for MscL from *E. coli* (5). The pressure at which MscL^{Ll} fully opened for the first time was determined and compared to the pressure at which MscS^{Ec} opened in giant spheroplasts from *E. coli* PB104. The pressure ratio of MscL^{Ll} / MscS^{Ec}, that is, the pressure at which MscL first opens fully relative to the pressure at which MscS^{Ec} opens in giant spheroplasts of *E. coli* PB104, was 1.81 ± 0.09 ($n = 20$). This means that there might be a small difference in the pressure sensitivity of MscL^{Ll} compared to MscL^{Ec}, which was found to have a MscL^{Ec} / MscS^{Ec} pressure ratio of 1.64 ± 0.08 (41). The open probability of MscL^{Ll} was determined by the average current (measured at a given pressure) divided by the current if all channels in the patch were open. The open probability was plotted against the pressure-ratio MscL / MscS^{Ec} and fitted to a Boltzmann distribution (Fig. 4C). Both MscL^{Ec} and MscL^{Ll} show initial openings around the same relative pressure. However, further opening of MscL^{Ll} required a higher energy input than opening of MscL^{Ec} as reflected by the different slopes of the sigmoidals (42). Finally, MscL^{Ll} appeared to have distinct substates at 0.26, 0.53 and 0.75 of full conductance (Fig. 4D), which compares to 0.22, 0.45, 0.70 and 0.93 of full opening for MscL^{Ec} (43).

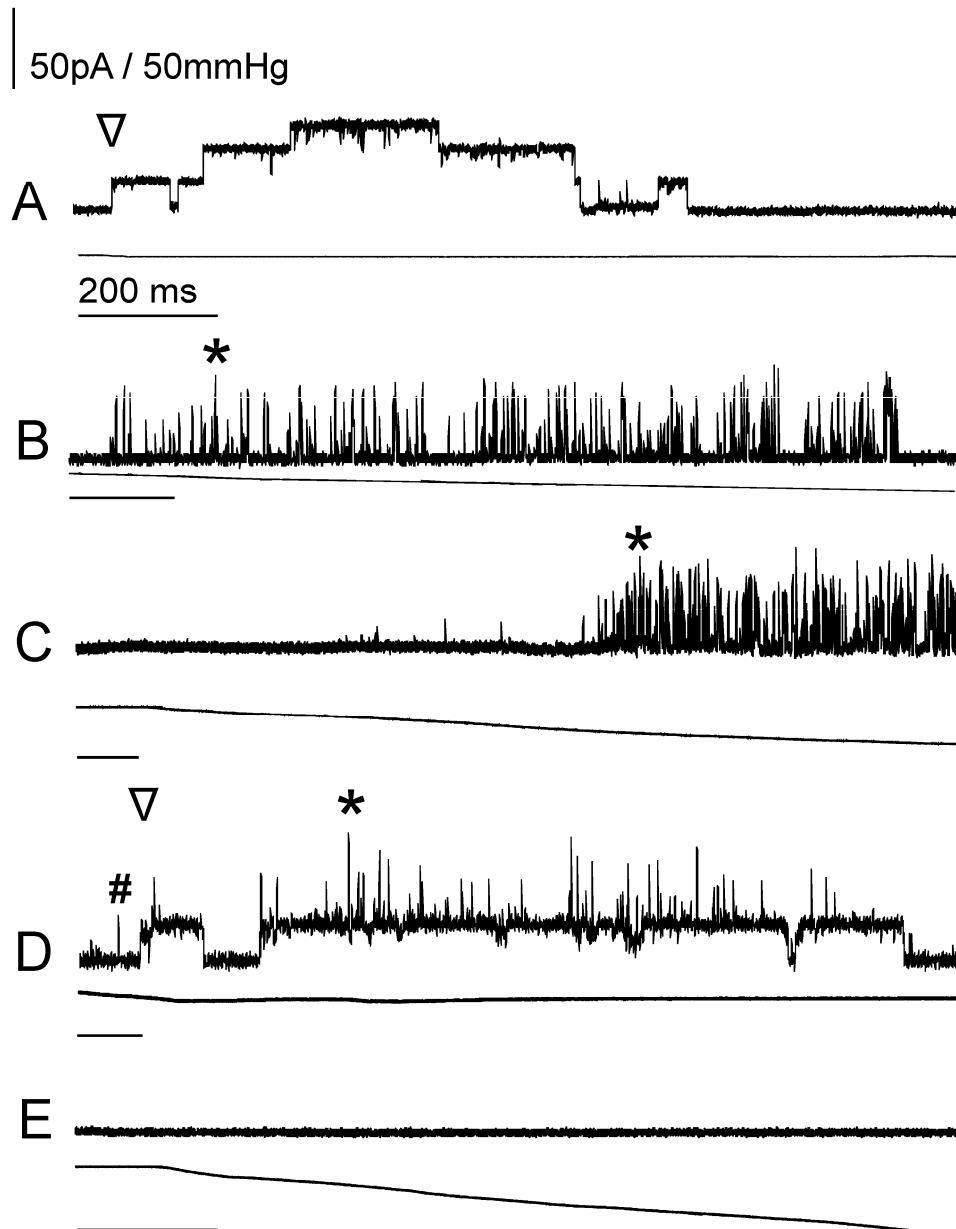


Figure 3: Typical electrophysiological recordings at 20mV (pipette) of patches excised from: (A) MJF465 spheroplasts expressing pBADyncB10H; (B) MJF465, pB10bmScL^{LI}6H spheroplasts; (C) IL1403 membranes fused with liposomes; (D) JIM7049, pNZ8048yncB10H membranes fused with liposomes; and (E) JIM7049 Δ MscL^{LI} membranes fused with liposomes. Top traces show current (bar corresponds to 50pA for all traces), bottom traces show applied suction pressure (bar corresponds to 150mmHg for all traces). Horizontal bars below traces indicate 2s for each trace. All traces start at 0mmHg pressure and 0pA current and were filtered in Clampfit 8.0 software (Axon Instruments, Foster City, USA) with the lowpass Boxcar filter at smoothing point 7. ∇ , first openings of MscS^{LI}, *, first full openings of MscL^{LI}, #, partial opening MscL^{LI}.

MscS^{Ll} and MscL^{Ll} in L. lactis. Channel activity in a patch excised from a hybrid proteo-GUV, prepared from *L. lactis* IL1403, is shown in Fig. 3C. MscL^{Ll}, but no MscS^{Ll} activity was observed in 30 independent patches. MscS^{Ll} activity was however observed in patches excised from hybrid proteo-GUVs from *L. lactis* JIM7049, over-expressing MscS^{Ll} (from pNZ8048yncB10H) as shown in Fig. 3D, indicating that the *yncB* gene product can be functional, but is possibly not expressed in wild-type *L. lactis*. The observation that MscS^{Ll} is apparently not functional in wild-type *L. lactis* is underscored by the observation that no MS channel activity whatsoever was observed in patches of JIM7049ΔMscL membranes fused with liposomes (n=10 with cells grown under low salt conditions; n=11 with cells grown under high salt conditions, Fig. 3E). Even if the native *L. lactis* JIM7049ΔMscL membrane to liposome ratio was increased 10-fold from 2:25 to 20:25 w/w (n=5, data not shown) MS channel activity was not observed. Recordings of channel activity of patches excised from proteoGUVs from *L. lactis* JIM7049 pNZ8048yncB10H, membranes expressing MscS^{Ll} were used to determine the pressure ratio for full openings of MscL^{Ll} relative to MscS^{Ll}. This value was 1.48 ± 0.05 (n=14), but substate channel activity of MscL^{Ll} could be observed before the first opening of MscS^{Ll} (e.g. # in Fig. 3D).

Cysteine mutants of MscL^{Ll} in E. coli. The cysteine mutants that had a GOF phenotype in response to MTSET labeling were analyzed with respect to the pressure ratio MscL^{Ll} / MscS^{Ec}, using *E. coli* PB104 expressing the channel from pB10bmscL^{Ll}6H (G20C) or pB10bmscL^{Ll}6H (V21C). Both G20C and G21C had a high pressure ratio of 2.6 ± 0.3 (n=8) and 3.7 ± 0.2 (n=4), respectively, in the absence of MTSET, but their activity became pressure independent upon addition of MTSET (data not shown).

Expression of *mscL*, *yncB* and *OpuAA*

As electrophysiological characterization of *L. lactis* IL1403 and JIM7049ΔMscL membranes, fused with liposomes, showed no MscS^{Ll} activity (Fig 3C), it seemed possible that *yncB* was not transcribed in these cells. RT-PCR was performed on RNA extracted from *L. lactis* IL1403 cells grown in CDM or CDM plus 0.5M NaCl and the resulting amplified DNA fragments were analyzed on gel (Fig. 5). After 15 PCR cycles, it is clearly visible that the transcription of *opuAA* (the first gene of the *opuA* operon) was increased in the cells grown at high salt (compare lane A3 with B3 in Fig. 5A), which is in agreement with a higher glycine betaine uptake capacity under these conditions (13). RT-PCR DNA corresponding to *mscL* and *yncB* fragments were visible after 22 PCR cycles. Both *mscL* and *yncB* are transcribed in wild-type *L. lactis* IL1403 cells, albeit to a low level compared to the *opuAA* gene of the *opuA* operon; the expression of the *mscL* and *yncB* was not significantly influenced by the osmolality of the medium (compare lane A1 with B1 and A2 with B2 in Fig. 5B). The negative controls showed that the extracted RNA was not contaminated with significant amounts of DNA as no product was obtained when reverse transcriptase was omitted from the reaction mixture (Fig. 5B; lanes A⁻ and B⁻); the lanes marked C1, C2 and C3

correspond to PCR products of *mscL^{Ll}*, *yncB* and *OpuAA*, respectively, using chromosomal DNA as template.

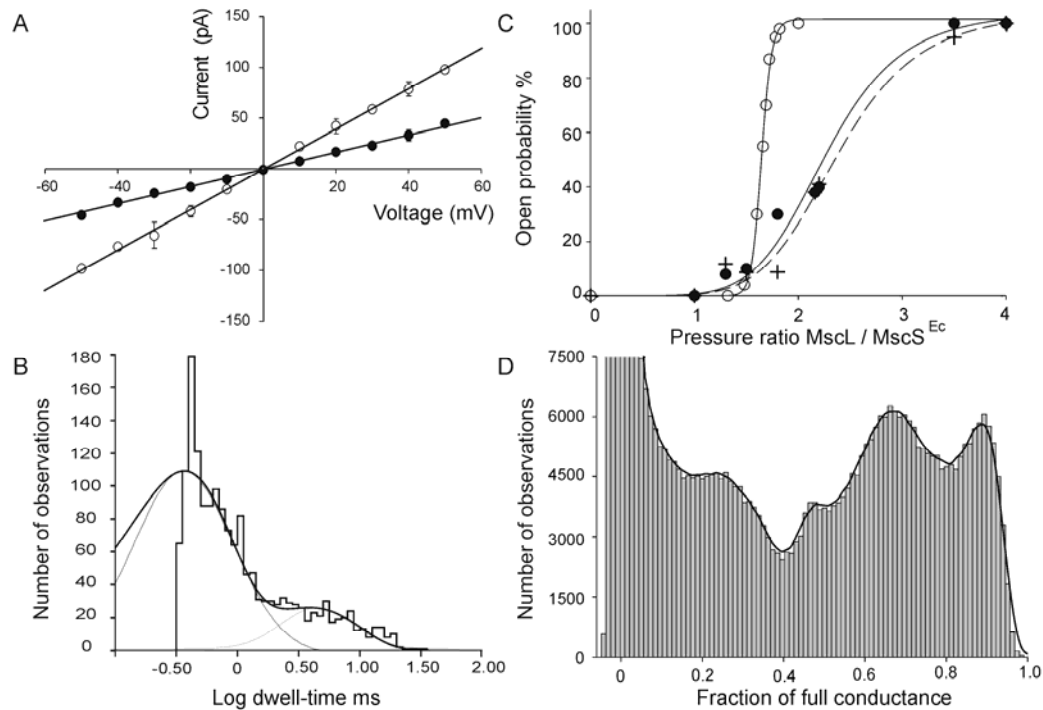


Figure 4: Characteristics of MscL^{Ll} and MscS^{Ll} (A) Current-Voltage relationship for MscL^{Ll} (○) and MscS^{Ll} (●), each based on three independent excised spheroplast patches. (B) Dwell time analysis of a single MscL^{Ll} trace obtained at -20mV with a two-component fit; fitted dwell times for this recording were 0.35 and 3.94ms. (C) Open probability at -20mV of MscL^{Ll} as a function of applied pressure: solid line; ●, based on mean current measurements, dashed line; + based on Popen analysis in Pstat software (Axon Instruments, Foster City, USA) and solid line; ○: open probability of MscL^{Ec} (based on data from 28). In all cases the open probabilities relative to the pressure required to open MscS^{Ec} are shown. Data for MscL^{Ll} was collected from 3 independent spheroplast patches with 1 – 3 channels per patch, in which MscL^{Ll} activity was saturated. (D) Relative conductive substates of MscL^{Ll} (compared to full opening) at -20mV determined by using an all-points histogram based on data from 5 independent patches. Data were normalized and the number of events per conductance substate was determined, from which the most frequently visited and therefore most stable substates were obtained.

Physiological characterization of JIM7049ΔMscL

Plasmid pOri280ΔMscL^{Ll} is not replicated in *L. lactis* JIM7049 unless it integrates into the chromosome, which preferentially takes place at the homologous position of the chromosomal *mscL* gene. By selecting for clones that grew in the presence of erythromycin, a disruption strain of *mscL* was obtained. MscL^{Ll} could not be detected by Western blot analysis in membranes of these cells, using antibodies raised against MscL^{Ll} (Fig. 2B).

To determine the role of MscL^{Ll} under conditions of hypo-osmotic stress, *L. lactis* IL1403 and JIM7049ΔMscL^{Ll} cells were grown on CDM supplemented with 365mM KCl. After washing in 50mM KPi plus 500mM KCl, pH 7.0, the cells were incubated with [¹⁴C]-glycine betaine for 40 minutes to allow internalization of the compatible solute and thereby compensate for the high external osmolality. A steady state level of uptake was attained, corresponding to an internal concentration of about 900nmol glycine betaine / mg total protein. The cells were then diluted into various hypotonic media and the fate of the internal glycine betaine content was determined. In Fig. 6A the internal concentrations are expressed as a percentage of the internal glycine betaine before osmotic downshift. The *L. lactis* IL1403 cells released ~80% of their glycine betaine when diluted 5-fold or more. The release of glycine betaine from *L. lactis* JIM7049ΔMscL was significantly lower; around 40% of the glycine betaine was retained by the cells. Taken as a whole, the data suggest that at least a fraction of the internalized glycine betaine is released via MscL^{Ll}.

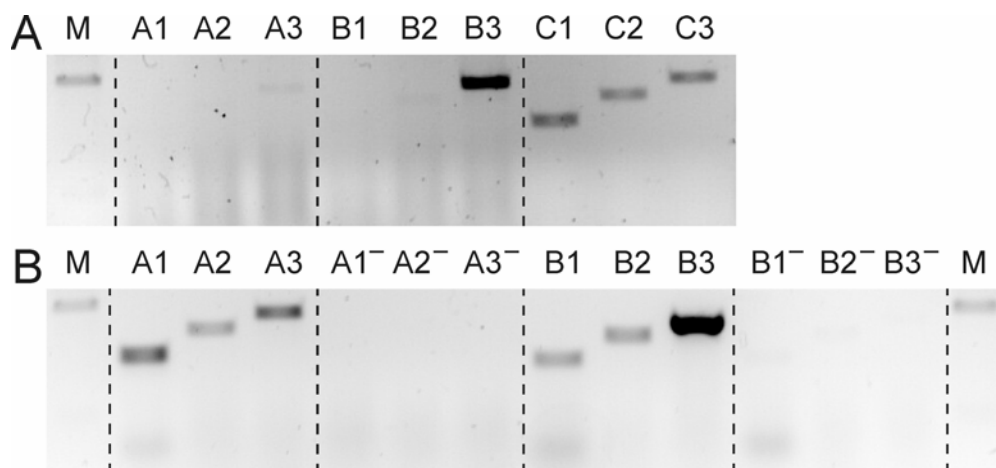


Figure 5: Analysis of RT-PCR products after (A) 15 cycles and (B) 22 cycles of amplification. Lanes A and B show RT-PCR products from RNA extracted from cells grown on CDM and CDM plus 0.5M NaCl, respectively, and lane C shows products from PCR on chromosomal DNA (positive control). Lanes A⁻ and B⁻ correspond to experiments with RNA samples not treated with AMV reverse transcriptase. For each condition (A, A⁻, B, B⁻ and C), lane 1 represents the presence or absence of a fragment from *mscL*^{Ll}; lane 2 represents the presence or absence of a fragment from *yncB* and lane 3 represents the presence or absence of a fragment from *opuAA*. Lanes marked with M show the 500 base-pair band of the lambda marker.

Next, cell survival was examined using protocols developed for *E. coli*. Under osmotic downshift conditions, 98 ±6% (n=3) of wild-type CFU survived and 80 ±5% (n=3) of the disruption strain. Because *L. lactis* grows in chains of mostly 2 or 4 cells, this could mean that in reality between 33 and 55% of the cells survive; to obtain a CFU from a chain of cocci it is sufficient if only a single cell is viable, see also Discussion section.

To obtain a quantitative measure of the consequences of an osmotic downshift on the metabolic activity of *L. lactis* IL1403 and JIM7049 Δ MscL, the capacity to ferment glucose was determined before and after osmotic downshift. Cells were grown in high salt medium and pre-loaded with glycine betaine and subjected to osmotic downshifts as described above. For *L. lactis* IL1403, only the metabolic activity after 100-fold dilution was determined, as even under this extreme downshift condition 100% of glucose metabolism was retained. In contrast, the rate of acidification of the buffer around *L. lactis* JIM7049 Δ MscL decreased with the fold dilution (Fig. 6B). The decrease in metabolic activity is quantitatively similar to the release of glycine betaine from JIM7049 Δ MscL, suggesting that the release of glycine betaine in the disruption mutant might be caused by loss of cell integrity rather than efflux through the MscL^{LI} channel.

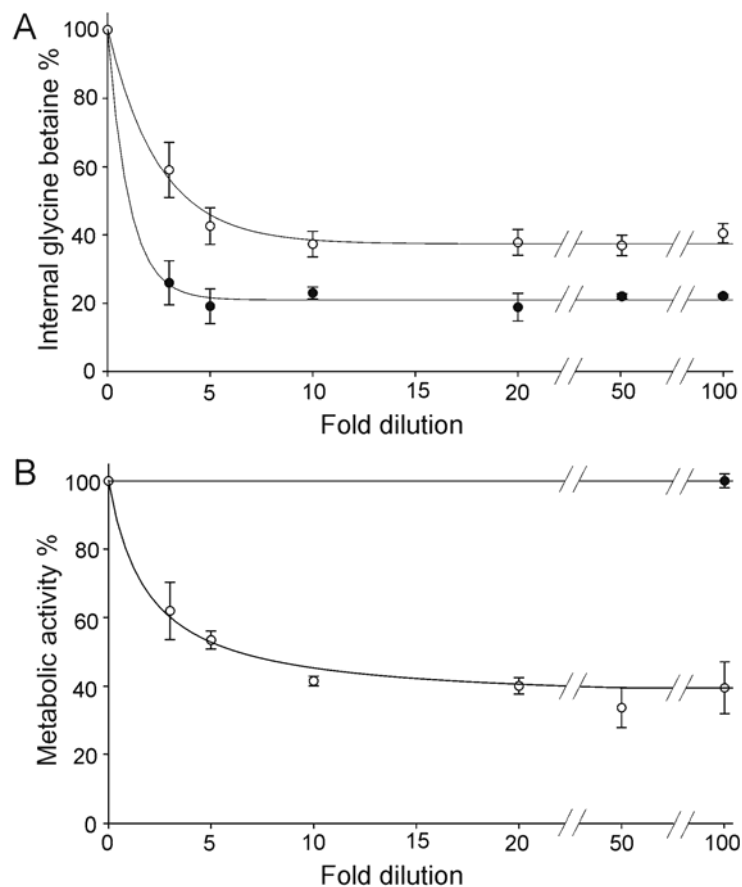


Figure 6: Glycine betaine efflux and metabolic activity of *L. lactis* IL1403 and JIM7049 Δ MscL upon osmotic downshift. (A) Release of [¹⁴C]-glycine betaine from IL1403 (●) and JIM7049 Δ MscL (○) cells; 100% values correspond to ~900nmol/mg of total protein. (B) Glucose fermentation activity of *L. lactis* IL1403 (●) and JIM7049 Δ MscL (○). Undiluted and 3, 5, 10, 20, 50 and 100-fold dilutions resulted in final osmolalities of 1050, 420, 295, 200, 155, 125 and 115mOsmol/kg, respectively. Values at "0-fold" dilution correspond to the values of the undiluted samples and were set to 100%. Metabolic activity at 100% corresponds to a pH change of 0.41 per hour per mg of total protein.

Discussion

MS channels of *L. lactis*

MscL and MscS from *L. lactis* form functional mechanosensitive channels when expressed in *E. coli* or *L. lactis*. Both channels provided *E. coli* MJF465 (MscS⁻ / MscL⁻) with protection against osmotic downshift as demonstrated in plate assays, and both channels were functional in patch-clamp experiments using membrane patches from *E. coli* spheroplasts, membrane patches from hybrid proteo-GUVs prepared from *L. lactis* membrane vesicles or membrane patches from proteo-GUVs prepared from purified and membrane-reconstituted protein. Importantly, in wild-type *L. lactis* only MscL^{L1} seems to be functional, and this MS channel appears critical for survival of the organism under conditions of hypo-osmotic stress.

The unitary conductances of MscS^{L1} and MscL^{L1} were 0.87nS and 2.0nS, respectively, which are within the range previously reported for MscS and MscL from other organisms (8, 9, 39). Open dwell times for MscL^{L1}6H were short compared to MscL^{Ec} and most other MscL homologues studied to date, giving rise to a "flickery" appearance in channel recordings. The activation thresholds of both *L. lactis* channels were comparable to those of the *E. coli* homologues as were the channel substates observed for MscL^{L1} (43). We also showed that MscL^{L1} could be activated by modifying cysteine residues with MTSET (G20C or V21C) at the constriction site of the pore, demonstrating that MscL from *L. lactis* functions very much like MscL from *E. coli*.

Survival and metabolic activity after osmotic downshift

Cell survival of *E. coli* MJF465 after osmotic downshift conditions was determined after heterologous expression of MscS^{L1} and MscL^{L1}. The experiments showed that both channels were able to partially rescue the MscL⁻ / MscS⁻ phenotype of the MJF465 strain. It can therefore be concluded that, in *E. coli*, both proteins form functional MS channels. In *L. lactis* it was harder to determine the effect of an osmotic downshift on cell survival because the cells grow in chains. The number of CFU of the disruption strain JIM7049ΔMscL decreased by 20% when the cells were subjected to an osmotic downshift. If a binomial distribution of cell death in a chain of 4 cells is assumed then the distribution of live and dead cells would be $L^4 + 4L^3D + 6L^2D^2 + 4LD^3 + D^4$ (where L stand for the fraction of live and D for the fraction of dead cells). As D^4 , *i.e.*, all cells in one chain are dead, is the only case that gives rise to a decrease in the number of CFU, the fraction of dead cells can be calculated as the fourth root of the fractional decrease in CFU. In this case the fraction of dead cells is $(0.20)^{1/4} = 0.67$, implying that only 33% of the cells survived the osmotic downshift. Assuming a chain length of two cells and a normal distribution, the survival would be 55%. With the most cells growing in chains of 2 and 4, the observed decrease in cell viability of 20% thus corresponds to an actual decrease in viability of 45-67%

The glucose fermentation capacity of *L. lactis* JIM7049ΔMscL decreased by 60% after osmotic downshift. Since the IL1403 wild-type strain (which normally expressed MscL^{L1}) was not affected by the osmotic downshift,

a fraction of the JIM7049 Δ MscL may have lysed, as a consequence of the inability to rapidly release osmolytes upon osmotic downshift. Strikingly, the decrease in glucose fermentation capacity of 60% compares well to the actual decrease in cell viability of 45-67%.

MscS activity is not detectable in wild-type *L. lactis*

Based on the following observations *L. lactis* IL1403 does not seem to possess detectable levels of functional MscS, even though the *yncB* gene is transcribed. Firstly, MscS^{LI} activity was not observed in patches excised from hybrid proteo-GUVs of IL1403, which displayed MscL activity. Secondly, MscS^{LI} activity was not observed in patches excised from hybrid proteo-GUVs of JIM7049 Δ MscL, which lacked any MS activity even when prepared from cells grown under different osmotic conditions. Finally, efflux of glycine betaine upon osmotic downshift was significantly decreased in JIM7049 Δ MscL. The residual 60% of efflux can be explained by cell lysis, as could be inferred from the decrease in CFU in the drop plate assay and the decrease in metabolic activity upon osmotic downshift. In contrast to *L. lactis*, an *E. coli* knockout strain released the same amount of glycine betaine as the wild-type *E. coli* upon osmotic downshift (44), suggesting that in *E. coli* another MS channel compensates for the absence of MscL or that in the wild-type strain MscL is not activated under the conditions used.

However, when *yncB* was expressed in *E. coli* MJF465 (using pBADyncB10H) or in *L. lactis* JIM7049 (using pNZ8048yncB10H) MS channel activity was observed. RT-PCR showed that the *yncB* gene is transcribed to levels comparable to *mscL* but much lower than *opuAA*. Moreover, and contrary to the *opuA* genes, the expression of *mscL* and *yncB* genes in *L. lactis* IL1403 does not seem to be influenced by the osmolality of the medium. In *E. coli* the expression of *mscL* and *mscS* is growth phase dependent and the transcription level of both genes increases when the osmolality of the medium increases (45). In analogy with MscS from *E. coli* one could argue that MscS from *L. lactis* is post-translationally inactivated; for instance, the open probability of MscS from *E. coli* is decreased by lowering of the pH and long exposures to membrane tension (12). Evidence for inactivation by prolonged exposure to membrane tension of MscS^{LI} can be observed in Fig. 3A (*yncB* expressed in *E. coli*), and it is possible that MscS in *L. lactis* IL1403 is kept in an inactive state, for which we have not been able to find the activation trigger. In contrast to wild-type *L. lactis*, overexpression of *yncB* in *L. lactis* yielded channel activity, suggesting that, when excess MscS channel is produced, a population of the molecules escapes the inhibition mechanism.

What are the consequences of inactive MscS for *L. lactis*? It is possible that MscS is less critical for *L. lactis* than for *E. coli*. Substate activity of MscL^{LI} can be observed at pressures at which MscS^{LI} is not yet observed. The presence of substates, together with the short dwell times of MscL^{LI}, may be sufficient for *L. lactis* to fine-regulate the internal osmolyte concentration without requiring a MscS-like activity.

In conclusion: MscS and MscL of *L. lactis* are genuine mechanosensitive channel proteins with properties similar to those described

for MscS and MscL from *E. coli*. We show, however, that MscL^{LI} is the primary, if not the only, mechanosensitive channel used by *L. lactis* under the conditions studied, through which a major portion of compatible solutes such as glycine betaine is released upon osmotic downshift.

Acknowledgements

We would like to thank MSC^{plus} for financial support, the Netherlands Organization for Scientific Research (NWO) for a travel grant (R88-247), Armağan Koçer (BioMaDe Technology Foundation) and the Neurobiophysics group of the University of Groningen for technical support with the electrophysiology experiments, and Sytse Henstra for assistance with the RT-PCR experiments. PB and PCM are supported by Grants GM61028 and DK60818 from the National Institutes of Health, Grant I-1420 of the Welch Foundation, and Grant F49620-01-1-0503 of the Air Force Office of Scientific Review. Strain MJF465 was kindly supplied by Prof. I.R.Booth, University of Aberdeen, UK.

Reference List

1. Hamill,O.P. and Martinac,B. (2001) *Physiol Rev.* **81**, 685-740
2. Wood,J.M., Bremer,E., Csonka,L.N., Kraemer,R., Poolman,B., van der,H.T., and Smith,L.T. (2001) *Comp. Biochem. Physiol. A Mol. Integr. Physiol.* **130**, 437-60.
3. Morbach,S. and Kramer,R. (2002) *Chembiochem.* **3**, 384-97
4. Poolman,B., Blount,P., Folgering,J.H.A., Friesen,R.H., Moe,P.C., and van der Heide,T. (2002) *Mol. Microbiol.* **44**, 889-902
5. Moe,P.C., Blount,P., and Kung,C. (1998) *Mol. Microbiol.* **28**, 583-92.
6. Maurer,J.A., Elmore,D.E., Lester,H.A., and Dougherty,D.A. (2000) *J. Biol. Chem.* **275**, 22238-44
7. Sukharev, S. I., Blount, P., Martinac, B., Blattner, F. R., and Kung, C. (1994) *Nature* **368**, 265-8
8. Sukharev,S.I., Martinac,B., Arshavsky,V.Y., and Kung,C. (1993) *Biophys. J.* **65**, 177-83
9. Ruffert, S., Berrier, C., Kramer, R., and Ghazi, A. (1999) *J. Bacteriol.* **181**, 1673-6
10. Chang,G., Spencer,R.H., Lee,A.T., Barclay,M.T., and Rees,D.C. (1998) *Science* **282**, 2220-6
11. Bass,R.B., Strop,P., Barclay,M., and Rees,D.C. (2002) *Science* **298**, 1582-7
12. Levina,N., Totemeyer,S., Stokes,N.R., Louis,P., Jones,M.A., and Booth,I.R. (1999) *EMBO J.* **18**, 1730-7
13. van der Heide,T. and Poolman,B. (2000) *J. Bacteriol.* **182**, 203-6
14. van der Heide,T., Stuart,M.C., and Poolman,B. (2001) *EMBO J.* **20**, 7022-32.
15. Poolman,B., Spitzer,J.J., and Wood,J.M. (2004) *Biochim. Biophys. Acta* **1666**, 88-104
16. Ou,X., Blount,P., Hoffman,R.J., and Kung,C. (1998) *Proc. Natl. Acad. Sci. USA* **95**, 11471-5
17. Yanisch-Perron,C., Vieira,J., and Messing,J. (1985) *Gene* **33**, 103-9
18. Chopin,A., Chopin,M.C., Moillo-Batt,A., and Langella,P. (1984) *Plasmid* **11**, 260-3
19. Gasson,M.J. (1983) *J. Bacteriol.* **154**, 1-9
20. de Ruyter,P.G., Kuipers,O.P., and de Vos,W.M. (1996) *Appl. Environ. Microbiol.* **62**, 3662-7
21. Drouault,S., Corthier,G., Ehrlich,S.D., and Renault,P. (2000) *Appl. Environ. Microbiol.* **66**, 588-98
22. Leenhouts,K., Buist,G., Bolhuis,A., ten Berge,A., Kiel,J., Mierau,I., Dabrowska,M., Venema,G., and Kok,J. (1996) *Mol. Gen. Genet.* **253**, 217-24
23. Alting-Mees,M.A. and Short,J.M. (1989) *Nucleic Acids Res.* **17**, 9494
24. Guzman,L.M., Belin,D., Carson,M.J., and Beckwith,J. (1995) *J. Bacteriol.* **177**, 4121-30

25. van der Does,C., den Blaauwen,T., de Wit,J.G., Manting,E.H., Groot,N.A., Fekkes,P., and Driessen,A.J. (1996) *Mol. Microbiol.* **22**, 619-29
26. Kuipers,O.P., de Ruyter,P.G.G.A., Kleerebezem,M., and de Vos,W.M. (1998) *Journal Of Biotechnology* **64**, 15-21
27. Poolman,B. and Konings,W.N. (1988) *J. Bacteriol.* **170**, 700-7.
28. Blount,P., Sukharev,S.I., Schroeder,M.J., Nagle,S.K., and Kung,C. (1996) *Proc. Natl. Acad. Sci. USA* **93**, 11652-7
29. Hamoen,L.W., Smits,W.K., de,J.A., Holsappel,S., and Kuipers,O.P. (2002) *Nucleic Acids Res.* **30**, 5517-28
30. Blount,P., Sukharev,S.I., Moe,P.C., Martinac,B., and Kung,C. (1999) *Methods Enzymol.* **294**, 458-82
31. Folgering,J.H.A., Kuiper,J.M., de Vries,A.H., Engberts,J.B.F.N., and Poolman,B. (2004) *Langmuir* **20**, 6985-7
32. Knol,J., Sjollema,K., and Poolman,B. (1998) *Biochemistry* **37**, 16410-5
33. Batiza,A.F., Kuo,M.M., Yoshimura,K., and Kung,C. (2002) *Proc. Natl. Acad. Sci. USA* **99**, 5643-8
34. Pearce,L.E. (1969) *N. Z. J. Dairy Sci. Technol.* **4**, 246-7
35. Laemmli,U.K. (1970) *Nature* **227**, 680-5
36. Schaffner,W. and Weissmann,C. (1973) *Anal. Biochem.* **56**, 502-14
37. van Montfort,B.A., Doeven,M.K., Canas,B., Veenhoff,L.M., Poolman,B., and Robillard,G.T. (2002) *Biochim. Biophys. Acta* **1555**, 111-5
38. Kunji,E.R., Slotboom,D.J., and Poolman,B. (2003) *Biochim. Biophys. Acta* **1610**, 97-108
39. Yoshimura,K., Batiza,A., and Kung,C. (2001) *Biophys. J.* **80**, 2198-206
40. Bartlett,J.L., Levin,G., and Blount,P. (2004) *Proc. Natl. Acad. Sci. U. S. A* **101**, 10161-5
41. Yoshimura,K., Batiza,A., Schroeder,M., Blount,P., and Kung,C. (1999) *Biophys. J.* **77**, 1960-72
42. Sukharev,S.I., Sigurdson,W.J., Kung,C., and Sachs,F. (1999) *J. Gen. Physiol.* **113**, 525-40
43. Chiang,C.S., Anishkin,A., and Sukharev,S. (2004) *Biophys. J.* **86**, 2846-61.
44. Ajouz, B., Berrier, C., Garrigues, A., Besnard, M., and Ghazi, A. (1998) *J. Biol. Chem.* **273**, 26670-4
45. Stokes,N.R., Murray,H.D., Subramaniam,C., Gourse,R.L., Louis,P., Bartlett,W., Miller,S., and Booth,I.R. (2003) *Proc. Natl. Acad. Sci. USA* **100**, 15959-64